View metadata, citation and similar papers at core.ac.uk
brought to you by CORE
provided by CERN Document Server

RADIATION DAMPING

R.P. Walker
Sincrotrone Trieste, Italy

Abstract
The basic formulae for the damping of the energy and betatron oscillations are derived. The results are applied to a number of examples of different lattice designs in which radiation damping effects are important. Methods of modifying and measuring the damping rates are also discussed.

1. INTRODUCTION

The loss of energy due to the emission of synchrotron radiation, and its replacement by the r.f. cavities, can give rise to a damping of the oscillations in energy and transverse displacement (synchrotron and betatron oscillations), a process known as "radiation damping". The only feature of the synchrotron radiation emission that is involved in this process is the rate of emission of energy, given in the previous Chapter on Synchrotron Radiation:

$$P = \frac{2}{3}\frac{e^2 c}{4\pi\varepsilon_0}\frac{\beta^4\gamma^4}{\rho^2} \tag{1}$$

From this can be obtained the total energy loss per turn, U_o, which in the case of an isomagnetic lattice (uniform bending radius in the bending magnets) is given by:

$$U_0 = \frac{e^2}{3\varepsilon_0}\frac{\beta^3\gamma^4}{\rho} \tag{2}$$

Because of the dependence on the fourth power of the rest mass the synchrotron radiation emission, and hence radiation damping effects, are only relevant for electrons at the energies of present-day accelerators. However, in the next generation of high energy proton accelerators the effects of radiation damping may start to become significant.

The process of radiation damping is important in many areas of electron accelerator operation:

i) it can give rise to a stable (Gaussian) distribution of transverse and longitudinal beam dimensions due to an equilibrium between the competing forces of radiation damping and "quantum excitation" – the growth of oscillation amplitudes due to the discrete emission of radiation quanta;
ii) it permits an efficient multi-cycle injection scheme to be employed in storage rings, by allowing the beam dimensions to damp in size between injection pulses;
iii) it allows large beam dimensions, produced in a linac for example, to be reduced in specially designed "damping rings";
iv) it helps to counteract beam growth due to various processes such as intra-beam scattering and collective instabilities.

In this chapter the basic formulae for the damping of the energy and betatron oscillations are derived, following closely the treatment in earlier texts [1–3]. The main results are illustrated by a number of examples of different lattice designs in which radiation damping effects are important. Methods of modifying the damping rates in a given ring are then discussed and finally techniques for the measurement of the damping rates are considered. The

following Chapter deals with the related quantum excitation process and the derivation of the equilibrium beam dimensions.

2. ENERGY OSCILLATIONS

Figure 1 shows the accelerating voltage, and hence the energy gain, in an r.f. cavity as a function of the time of arrival of an electron. The particle which arrives on every turn at the correct time (and hence phase with respect to the r.f. voltage) in order to make up the loss due to synchrotron radiation (U_0) is called the synchronous particle, and its energy is the nominal energy of the design orbit, E_0 An electron with a higher energy will in general travel on a longer path and therefore arrive later at the cavity. It can be seen from Fig. 1 that such a particle will receive less energy at the cavity, which therefore compensates for the energy deviation. Similarly, a lower energy particle travels on a shorter path, arrives earlier at the cavity and therefore has a higher energy gain. This describes the usual stable oscillations in energy and time that occur about the synchronous point, which are analysed in more detail in Ref. [4]. If in addition the energy loss due to synchrotron radiation increases with the energy of the particle, then it can be seen that this will provide a damping of the oscillations.

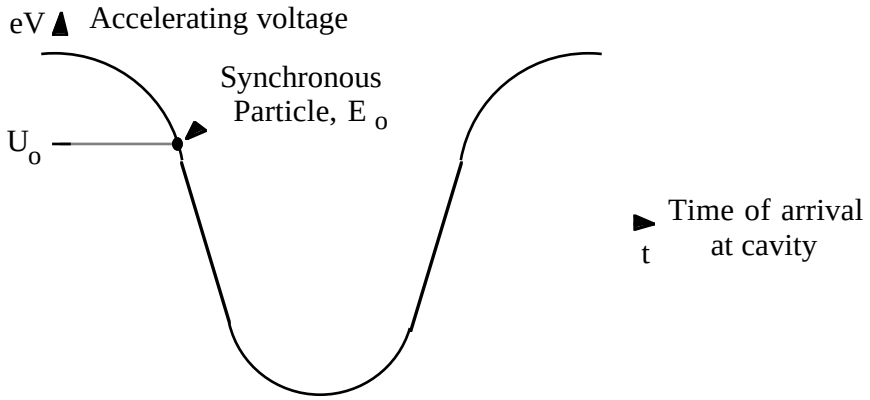

Fig. 1 Variation of accelerating voltage in an r.f. cavity as a function of electron arrival time

We now consider this damping process in more detail. The standard terminology will be used which refers to the time displacement of an electron with respect to the synchronous particle, or equivalently to the centre of the bunch, as shown in Fig. 2. In this description an electron which is ahead of the synchronous electron by a distance Δs has a positive time displacement $\tau = \Delta s/c$. An electron with a positive energy deviation $\varepsilon = E\text{-}E_0$ has a larger orbit length (L) and hence orbit period (T) with respect to the synchronous particle (denoted by the subscript o) given by:

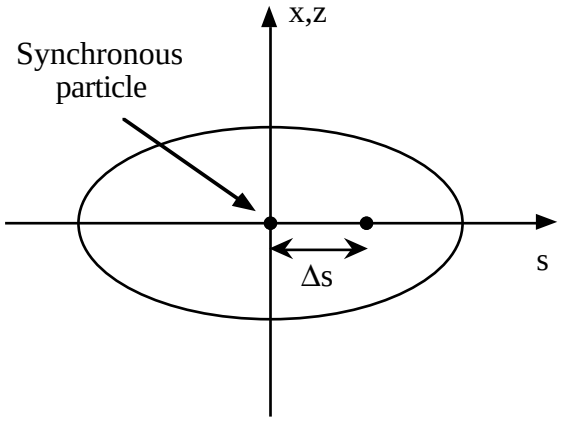

Fig. 2 Location of the synchronous particle and an electron with a positive time displacement in an electron bunch

$$\frac{\Delta T}{T_0} = \frac{\Delta L}{L_0} = \alpha \frac{\varepsilon}{E_0}$$

where α is the momentum compaction factor, neglecting the relativistic factor which is negligible for electrons [4]. We assume that changes in energy and time displacement occur slowly with respect to the orbit period, which permits use of a differential notation:

$$\frac{d\tau}{dt} = - \alpha \frac{\varepsilon}{E_0} \tag{2}$$

Considering the energy equation, in one turn an electron loses an energy $U(\varepsilon)$ and gains from the r.f. cavity $eV(\tau)$; the net change is therefore:

$$\Delta E = eV(\tau) - U(\varepsilon)$$

and so on average:

$$\frac{d\varepsilon}{dt} = \frac{eV(\tau) - U(\varepsilon)}{T_0}$$

Taking the derivative of the above then gives:

$$\frac{d^2\varepsilon}{dt^2} = \frac{e}{T_0}\left(\frac{dV(\tau)}{d\tau}\frac{d\tau}{dt}\right) - \frac{1}{T_0}\left(\frac{dU(\varepsilon)}{d\varepsilon}\frac{d\varepsilon}{dt}\right)$$

Inserting Eq. (2) gives:

$$\frac{d^2\varepsilon}{dt^2} + \frac{1}{T_0}\frac{dU(\varepsilon)}{d\varepsilon}\frac{d\varepsilon}{dt} + \frac{e}{T_0}\frac{\alpha}{E_0}\frac{dV(\tau)}{d\tau}\varepsilon = 0 \tag{3}$$

For small oscillations it can be assumed that the accelerating voltage varies linearly with respect to the arrival time around that of synchronous particle:

$$eV(\tau) = U_0 + e\dot{V}_0 \tau$$

where $\dot{V}_0$ is the slope of the accelerating voltage $dV(\tau)/d\tau$ at $\tau = 0$. Using this expression Eq. (3) can be written as follows:

$$\frac{d^2\varepsilon}{dt^2} + 2\alpha_\varepsilon \frac{d\varepsilon}{dt} + \Omega^2\varepsilon = 0$$

where:

$$\alpha_\varepsilon = \frac{1}{2T_0}\frac{dU}{d\varepsilon} \tag{4}$$

$$\Omega^2 = \frac{e}{T_0}\dot{V}_0\frac{\alpha}{E_0}$$

This can be recognised as the usual equation of harmonic motion for the energy oscillations [4] with an additional damping term. Assuming that the damping rate α_ε is small with respect to the oscillation frequency Ω, the solution can be written as follows:

$$\varepsilon(t) = A\, e^{-\alpha_\varepsilon t} \cos(\Omega t - \phi)$$

$$\tau(t) = \frac{-\alpha}{E_0\Omega} A e^{-\alpha_\varepsilon t} \sin(\Omega t - \phi)$$

where A and ϕ are constants determined by the initial conditions. It can be seen that as anticipated the damping rate depends on the change in energy loss with energy deviation $(dU(\varepsilon)/d\varepsilon)$.

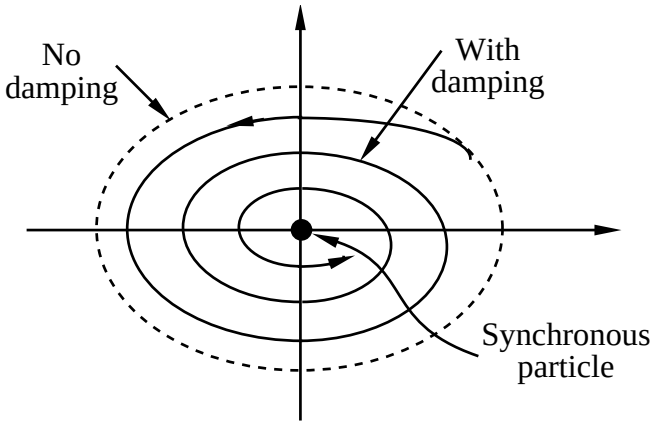

Fig. 3 Illustration of energy oscillations with and without radiation damping

Figure 3 illustrates the above solutions. In the absence of damping an electron executes a harmonic oscillation in energy and time with a fixed amplitude that is represented by an ellipse of a given size. With positive damping the particle spirals slowly towards the fixed point, namely the synchronous particle.

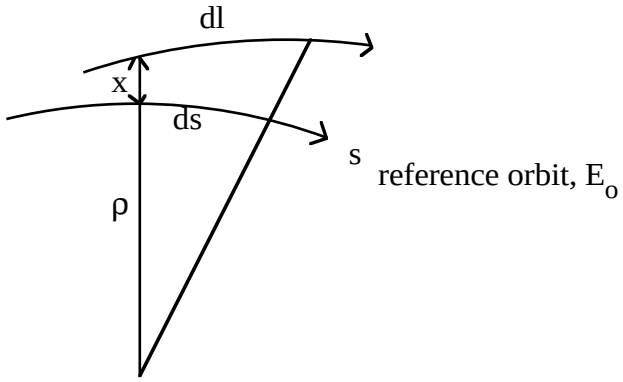

Fig. 4 Elements of the reference orbit and a displaced trajectory

We now consider how to calculate the damping rate (α_ε) from the rate of change of energy loss with energy ($dU/d\varepsilon$). When the energy deviates from the nominal energy E_0 the energy loss changes because of several factors. Firstly, the energy loss is itself a function of energy and secondly because the orbit deviates from the reference orbit there may be a change in magnetic field and a change in the path length. Figure 4 shows a curved element of the design orbit in the horizontal plane for a particle of the nominal energy E_0, where the radius of curvature is ρ. Also shown is the trajectory of another particle with transverse displacement, x. In general the path length for the elements are related as follows:

$$\frac{dl}{ds} = 1 + \frac{x(s)}{\rho} \tag{5}$$

For an off-energy particle the closed orbit is defined by:

$$x(s) = D(s)\,\frac{\varepsilon}{E_0} \tag{6}$$

where $D(s)$ is the dispersion function. In this case therefore:

$$\frac{dl}{ds} = 1 + \frac{D}{\rho}\,\frac{\varepsilon}{E_0} \tag{7}$$

The energy radiated per turn is defined as the integral of the radiated power (P) around the off-energy orbit:

$$U(\varepsilon) = \frac{1}{c}\oint P\,dl$$

Using Eq. (7) for the path length this can be expressed as an integral over s:

$$U(\varepsilon) = \frac{1}{c}\oint P\left(1 + \frac{D}{\rho}\frac{\varepsilon}{E_0}\right)ds$$

We now expand P as a function of energy and transverse displacement, given the fact that P is proportional to E^2 and $B^2(x)$, Eq. (1):

$$P(s) = P_0 + \frac{2P_0}{E_0}\,\varepsilon + \frac{2P_0}{B_0}\,\frac{dB}{dx}\,x \tag{8}$$

where $P_0(s)$ is the power radiated on the design orbit, corresponding to the field B_0. Inserting in the expression for $U(\varepsilon)$ together with Eq. (6) and keeping only linear terms in ε we obtain:

$$U(\varepsilon) = \frac{1}{c}\oint\left(P_0 + \frac{2P_0}{E_0}\varepsilon + \frac{dB}{dx}D\frac{\varepsilon}{E_0} + \frac{P_0 D}{\rho}\frac{\varepsilon}{E_0}\right)ds$$

For the damping rate we require the derivative:

$$\frac{dU(\varepsilon)}{d\varepsilon} = \frac{1}{c}\oint\left(\frac{2P_0}{E_0} - \frac{2P_0 k\rho D}{E_0} + \frac{P_0 D}{\rho E_0}\right)ds$$

where the usual focusing parameter k for gradient fields has been introduced ($k\rho = [-dB/dx]/B_0$). Since the integral of P_0/c around the design orbit is U_0, we obtain:

$$\frac{dU(\varepsilon)}{d\varepsilon} = \frac{2U_0}{E_0} + \frac{1}{cE_0}\oint P_0 D\left(1/\rho - 2k\rho\right)ds$$

and hence the equation for the damping rate can be expressed in the following standard form:

$$\alpha_\varepsilon = \frac{1}{2T_0}\,\frac{dU}{d\varepsilon} = \frac{1}{2T_0}\,\frac{U_0}{E_0}\,(2+D)$$

where:

$$D = \frac{1}{cU_0}\oint P_0 D\left(1/\rho - 2k\rho\right)ds \tag{9}$$

Using the fact that P_0 depends on $1/\rho^2$, the important parameter D can be expressed in the following standard forms, involving only integrals over various lattice functions:

$$D = \frac{\oint D/\rho\left(1/\rho^2 - 2k\right)ds}{\oint 1/\rho^2 ds} = \frac{\oint D(1-2n)/\rho^3 ds}{\oint 1/\rho^2 ds} \tag{10}$$

It is clear that D is a dimensionless number, with contributions only from the ring bending magnets ($1/\rho \neq 0$). One term involves both bending and focusing fields ($k/\rho \neq 0$) which is present in "combined function" or "synchrotron magnets". For these magnets it is convenient to define a field index, n:

$$n = -\frac{dB}{dx}\frac{\rho}{B_0} = k\rho^2$$

which appears in the second expression above for D.

From the expression for the damping rate, Eq. (4), we recall that $dU/d\varepsilon$ must be positive for the oscillations to be damped and hence $D > -2$. In the most common case of a "separated function" lattice (as will be seen later) D is a small positive number, in which case dU/dε is determined only by the E^2 dependence of P. In this case we have the result that:

$$\tau_\varepsilon = \frac{1}{\alpha_\varepsilon} \approx \frac{T_0\, E_0}{U_0} \tag{11}$$

i.e. the damping time is approximately the time it would take for an electron to radiate away all its energy (at constant rate), a useful and easily remembered result.

We conclude this section with a table giving various parameters connected with the energy oscillations for two widely different electron machines at CERN, the EPA [5] and LEP [6]. It can be seen that in both cases the damping time is much longer than the synchrotron oscillation and orbit periods, justifying the approximations used in the derivation above. Finally, we note that for protons even at the high energy expected at the SSC (20 TeV) the damping time is still extremely long, about 12 hours.

Table 1

Energy oscillation parameters for two electron storage rings

	EPA [5]	LEP [6]
Energy, E_0(GeV)	0.6	55
Energy loss per turn, U_0 (keV)	8	$260\ 10^3$
Orbit period, T_0(μs)	0.42	89
Synchrotron oscillation period (ms)	0.27	1
Synchrotron oscillation damping time, τ_ε (ms)	64	18

3. BETATRON OSCILLATIONS

We consider now the damping of the betatron oscillations, starting with the more simple case of the vertical plane.

3.1 Vertical plane

It is convenient to use the following approximate form for the vertical betatron oscillations:

$$z = A\cos(\phi(s) + \phi_0) \qquad z' = \frac{-A}{\beta}\sin(\phi(s) + \phi_0)$$

where A is the normalised amplitude of the oscillation:

$$A^2 = z^2 + (\beta z')^2 \tag{12}$$

However, it is easy to show that the same result is obtained if the complete form for the amplitude is used:

$$A^2 = \gamma z^2 + 2\alpha z z' + \beta z'^2$$

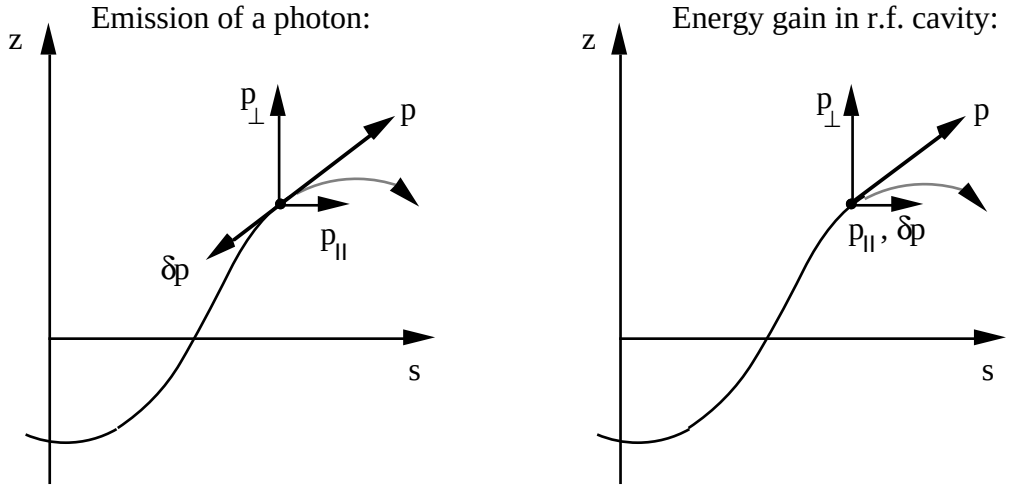

Fig. 5 Effect of energy loss and energy gain processes on the electron momentum

We wish to consider the effect on the oscillation amplitude A of energy loss due to synchrotron radiation and energy gain in the r.f. cavities. These processes are illustrated in Fig. 5, occurring at an arbitrary point with respect to the phase of the betatron oscillation. It can be seen that since photons are emitted in the direction of the motion of the electron, there is a change in the value of the momentum, but no change in angle z'. On the other hand, in the r.f. cavity there is an increase in the longitudinal component of the momentum ($p_{||}$) which therefore reduces the angle. Since $z' = p_\perp/p_{||}$, after the cavity we have

$$z' + \delta z' = \frac{p_\perp}{p_{||} + \delta p} \approx z'\left(1 - \frac{\delta p}{p}\right)$$

and hence:

$$\delta z' = -z'\frac{\delta\varepsilon}{E_0}$$

Using Eq. (12) the change in oscillation amplitude is given by:

$$A\,\delta A = \beta^2 z'\,\delta z' = -\beta^2 z'^2\frac{\delta\varepsilon}{E_0}$$

Averaging over all possible phases of the oscillation at the time the electron passes through the cavity, $\langle z'^2\rangle = A^2/2\beta$, we have:

$$\frac{<\delta A>}{A} = -\frac{1}{2}\frac{\delta\varepsilon}{E_0}$$

Since the gain in energy over one turn is small compared to the electron energy we can average over one turn to obtain:

$$\frac{\Delta A}{A} = \frac{-U_0}{2\,E_0} \tag{13}$$

The motion is therefore exponentially damped (exp - $\alpha_z t$) with a time constant α_z given as follows:

$$\alpha_z = -\frac{1}{A}\frac{dA}{dt} = \frac{U_0}{2\,E_0\,T_0}$$

which is one half of the approximate value for the energy oscillations derived in the previous section, Eq. (11).

3.2 Horizontal plane

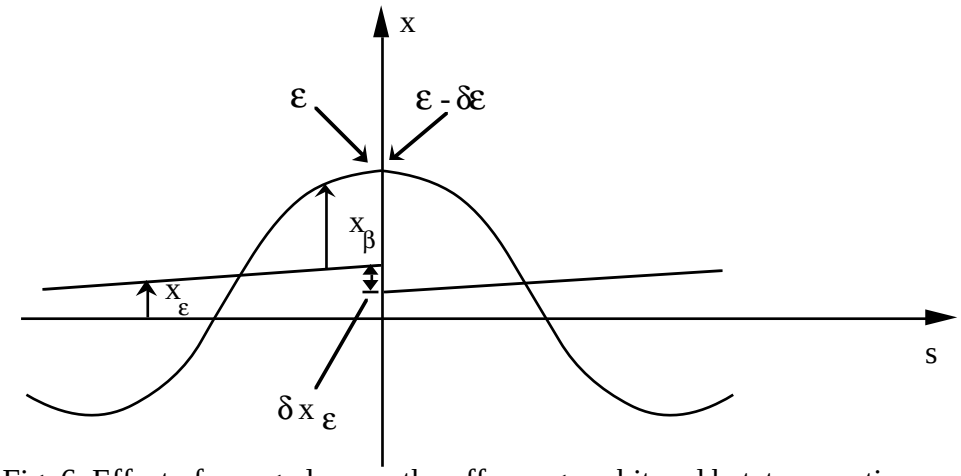

Fig. 6 Effect of energy loss on the off-energy orbit and betatron motion in the horizontal plane

The same process as above occurs in the horizontal plane also, but there is an additional effect due to the emission of synchrotron radiation at points where there is finite dispersion (which is usually zero in the vertical plane). As before, there is no change in x or x' due to the radiation emission (see Fig. 6), however the change in energy implies a change in the off-energy orbit ($x_\varepsilon = D(s)\,\varepsilon/E_0$) and hence an equal and opposite change in the betatron amplitude x_β, since $x = x_\varepsilon + x_\beta$. We have therefore:

$$\delta x_\beta = -\delta x_\varepsilon = -D\frac{\delta\varepsilon}{E_0}$$

Similarly, the change in angle of the betatron oscillation is given by:

$$\delta x_\beta' = -\delta x_\varepsilon' = -D'\frac{\delta\varepsilon}{E_0}$$

The change in the oscillation amplitude A where:

$$A^2 = x_\beta^2 + \left(\beta\, x_\beta'\right)^2$$

is therefore given as follows:

$$A\,\delta A = x_\beta\,\delta x_\beta + \beta^2\, x'_\beta\;\delta x'_\beta = -\,(D\,x_\beta + \beta^2\, D'\, x'_\beta)\;\frac{\delta\varepsilon}{E_0} \qquad (14)$$

If the rate of energy loss were constant then averaging over the betatron phase would yield no net increase in amplitude, however, this is not the case and it is necessary to include the variation of energy loss with x_β. Since the energy loss in a small element is given by $\delta\varepsilon = -P/c\;\delta l$, where (Eq. (5)):

$$\frac{\delta l}{\delta s} = 1 + \frac{x_\beta}{\rho}$$

and expressing P as a function of x_β, as in Eq. (8):

$$P = P_0 + \frac{2P_0}{B_0}\,\frac{dB}{dx}\;x_\beta = P_0\,(1 - 2k\rho x_\beta)$$

gives the result:

$$\delta\varepsilon = -\frac{P_0}{c}\left(1 - 2k\rho x_\beta + \frac{x_\beta}{\rho}\right)\delta s$$

Combining with Eq. (14) and averaging over the betatron phase, given that $\langle x_\beta\rangle = 0$, $\langle x'_\beta\rangle = 0$, $\langle x_\beta x'_\beta\rangle = 0$, and $\langle x_\beta^2\rangle = A^2/2$ gives:

$$\frac{\langle\delta A\rangle}{A} = \frac{P_0}{2cE_0}\;D\,(1/\rho - 2k\rho)\;\;\delta s$$

Over one turn therefore:

$$\frac{\Delta A}{A} = \frac{1}{2cE_0}\oint P_0 D\left(1/\rho - 2k\rho\right)ds = \frac{U_0}{E_0}\frac{D}{2}$$

using the earlier definition of the quantity D, Eq. (9).

In general, since D is usually positive, this would give rise to an increase in oscillation amplitude, however when the effect of the damping that occurs due to the energy gain in the r.f. cavities is added, as in the vertical plane Eq. (13), we have:

$$\frac{\Delta A}{A} = \frac{-U_0}{2E_0}\,(1\text{-}D)$$

and hence the damping rate is as follows:

$$\alpha_x = -\frac{1}{A}\,\frac{dA}{dt} = \frac{U_0}{2\,E_0\,T_0}\,(1\text{-}D) \qquad (15)$$

3.3 Origin of the damping of the betatron motion

It is interesting to note that the main damping effect of the betatron motion described in section 3.1 appears to occur due to the energy gain in the r.f. cavities, not due to the energy loss, and as a result it has been remarked that the term "radiation damping" is somewhat

inappropriate. However, it can be seen from Fig. 5 that in fact the opposite is true if the canonically conjugate variables of position and momentum are used rather than the more usual position and angle , since the transverse momentum, $p_\perp$, is reduced when a photon is emitted but is unchanged in the r.f. cavity [7]. The choice of variables therefore determines the apparent location of the damping effect, however the final result is the same.

4. DAMPING PARTITION AND THE ROBINSON THEOREM

The results obtained in the previous two sections may be summarized as follows:

$$\alpha_i = \frac{J_i U_0}{2 E_0 T_0} \tag{16}$$

where i represents x, z or ε and J_i are the Damping Partition Numbers:

$$J_x = 1\text{-}D \qquad J_z = 1 \qquad J_\varepsilon = 2\text{+}D$$

so called because the sum of the damping rates for the three planes is a constant:

$$J_x + J_z + J_\varepsilon = 4 \tag{17}$$

a result known as the Robinson Theorem [8]. For damping in all planes simultaneously it is required that all $J_i > 0$ and hence that $-2 < D < 1$.

We have obtained the above result for the total damping explicitly by analysing each oscillation mode independently, however it may be obtained in a more general and direct way using the following method [8]. The general transverse and longitudinal motion of a particle with respect to that of the synchronous particle on the design orbit may be described using 6x6 transfer matrices, relating particle coordinates at some initial position s_1 to those at some later position s_2 as follows:

$$\begin{bmatrix} x \\ x' \\ z \\ z' \\ \varepsilon/E_0 \\ \tau \end{bmatrix}_{s_2} = \begin{bmatrix} \\ \mathbf{M}\,(s_2, s_1) \\ \\ \end{bmatrix} \begin{bmatrix} x \\ x' \\ z \\ z' \\ \varepsilon/E_0 \\ \tau \end{bmatrix}_{s_1}$$

Since the elements of $\boldsymbol{M}$ are real then the eigenvalues of the one-turn matrix $\boldsymbol{M}(s + L, s)$ can be written as three complex conjugate pairs $\exp(-\alpha'_j \pm i\beta'_j)$ with $j = 1,2,3$. Using the fact that the determinant of a matrix is the product of its eigenvalues [9] we have:

$$\det \boldsymbol{M}(s+L,s) = \exp\left(-\sum_{j=1}^{3} 2\alpha'_j\right) \cong 1 - \sum_{j=1}^{3} 2\alpha'_j \tag{18}$$

since $\alpha'_j << 1$. The amplitudes of the three oscillation modes vary as $\exp(-\alpha_j t)$ where $\alpha_j = \alpha'_j / T_0$ i.e. α_j are the damping rates.

Considering a general infinitesimal element of orbit between s and $s+ds$, the matrix can be written:

$$\boldsymbol{M}\,(s+ds,s) = \boldsymbol{I} + \delta\boldsymbol{M}$$

where $\boldsymbol{I}$ is the identity matrix. Since all elements of $\delta\boldsymbol{M}$ are small, it can be shown that:

$$\det \boldsymbol{M}\,(s+ds,s) \approx 1 + T_r\,(\delta \boldsymbol{M})$$

where T_r represents the trace of the matrix. In the absence of energy loss and gain the determinant of $\boldsymbol{M}$ is equal to unity. The only diagonal terms in $\delta\boldsymbol{M}$ therefore are those calculated earlier representing changes in x' and z' due to gain of energy $\delta\varepsilon_1$:

$$\delta x' = -\frac{\delta\varepsilon_1}{E_0}\, x' \quad , \quad \delta z' = -\frac{\delta\varepsilon_1}{E_0}\, z'$$

as well as that for ε/E_0 due to energy loss:

$$\delta\varepsilon = -2\frac{\delta\varepsilon_2}{E_0}\, \varepsilon$$

since the rate of emission is proportional to E^2. We have therefore:

$$\det \boldsymbol{M}\,(s+ds,s) = 1 - 2\frac{\delta\varepsilon_1}{E_0} - 2\frac{\delta\varepsilon_2}{E_0}$$

For the one-turn matrix, since the determinant of a product of matrices is the product of the determinants and since the total energy gain and the total energy loss are equal to U_0, we have that:

$$\det \boldsymbol{M}(s+L,s) = 1 - \frac{4\,U_0}{E_0}$$

irrespective of the location of the energy loss and gain. Combining with Eq. (18) gives the final result:

$$\sum_{j=1}^{3} \alpha_1 = \frac{2}{E_0}\frac{U_0}{T_0}$$

which is identical to the one obtained earlier, Eqs. (16) and (17). The present derivation however shows that the result is independent of the nature of the magnetic and electric field distributions acting on an electron, provided that they are determined *a priori*, i.e no beam induced fields are included. It is valid therefore even in the case of linear coupling between the horizontal and vertical planes, and when there is bending in the vertical plane. In the absence of these factors the matrices for the (z,z') and $(x,x',\varepsilon/E_0,\tau)$ motion and may be treated separately, giving the result:

$$\alpha_x + \alpha_\varepsilon = \frac{3\,U_0}{2\,E_0\,T_0}$$

or equivalently,

$$J_x + J_\varepsilon = 3.$$

5. RADIATION DAMPING ASPECTS IN VARIOUS LATTICE DESIGNS

5.1 Weak focusing lattices

Early accelerators employed "weak focusing" magnets that provided focusing in both planes simultaneosly for which the field index must lie in the range $0 < n < 1$ [10]. There is a

further constraint on the field index in order that the motion is damped in all three planes. To derive this we first write the expression for D in a form that is valid in the case of an isomagnetic lattice:

$$D = \frac{1}{2\pi p}\oint(1-2n)\frac{D}{\rho}ds \tag{19}$$

We leave ρ inside the integral to indicate that it includes only the bending magnets and not any straight sections. We can simplify this by making use of the expression that defines the dispersion function:

$$D'' = \left(k - \frac{1}{\rho^2}\right)D + \frac{1}{\rho}$$

from which it follows by integration that:

$$\oint\left(1/\rho^2 - k\right)Dds = \oint(1/\rho)ds$$

If the focusing is due entirely to combined function magnets, with field index $n = k\rho^2$, then the above may be written in the isomagnetic case as follows:

$$\oint(1-n)\frac{D}{\rho} = 2\pi\rho \tag{20}$$

If we now include the fact that the field index is also constant in the bending magnets, then combining Eqs. (19) and (20) gives:

$$D = \frac{1\text{-}2n}{1\text{-}n}$$

It follows that the damping partition numbers are then given by:

$$J_x = \frac{n}{1\text{-}n} \qquad J_z = 1 \qquad J_\varepsilon = \frac{3\text{-}4n}{1\text{-}n}$$

and so for damping in all three planes $0 < n < 0.75$. The fact that energy oscillations become undamped for $n > 0.75$ was appreciated even before the first observation of synchrotron radiation [11-13].

A present day example of this type of lattice is the NBS 250 MeV storage ring which is used as a synchrotron radiation facility (SURF). Originally however the ring was operated as a 180 MeV synchrotron with a field index of 0.8; when it was converted for use as a storage ring extra gradient coils were added to lower the field index to 0.6 in order to obtain the necessary damping of all oscillation modes [14]. A more recent example is the compact superconducting synchrotron radiation source AURORA whose field index varies in the range 0.3–0.7 as the energy is varied between 150 and 650 MeV [15].

5.2 Strong focusing, combined function

Several early types of alternating gradient or "strong focusing", synchrotrons were constructed using magnets with combined bending and focusing fields, for example the CEA and DESY I electron synchrotrons, as well as the PS proton synchrotron. If there are no separate focusing fields ($k \neq 0$ only if $1/\rho \neq 0$) then combining Eqs. (19) and (20) above, gives in the isomagnetic case:

$$D = 2 - \frac{\oint (D/\rho) ds}{2\pi\rho} = 2 - \frac{\alpha L}{2\pi\rho}$$

where α is the momentum compaction factor. Since α is usually small it may be seen that $D \sim 2$ and hence $J_x \sim -1$, $J_z = 1$ and $J_\varepsilon \sim 4$. In the case of a combined function lattice therefore the betatron motion is anti-damped in the horizontal plane [16–18]. Electron synchrotrons can however be built with a combined function lattice, provided the growth that occurs in the horizontal beam size is acceptable.

In order to overcome the anti-damping of the combined function lattice various correction methods have been proposed [8,16,17,19,20], some of which are discussed in Section 6.

5.3 Strong focusing, separated function

It has been shown that radial damping can be achieved in a combined function lattice by using focusing and defocusing magnets of slightly different strength [8, 21]. The most common lattice arrangement however which produces damping in all three planes, is the so-called separated function lattice i.e. one in which the functions of bending and focusing are divided in separate dipole and quadrupole magnets [22,23]. One possibility may be seen directly from Eq. (10). It is clear that with a value of $n = 0.5$ in the bending magnets $D = 0$, and hence $J_x = J_z = 1$, $J_\varepsilon = 2$, irrespective of additional quadrupole magnets which may be arranged to produce an alternating gradient structure. Such an approach was taken in the design of both the ACO and ADONE storage rings.

In the case of zero field gradient in the dipole magnets, it may be seen from Eq. (10) that in the isomagnetic case we have:

$$D = \frac{\oint (D/\rho) ds}{2\pi\rho} = 2 - \frac{\alpha L}{2\pi\rho}$$

The value of D in this case results only from the path length effect in the dipole magnets, which is usually very small. In all of the above analysis we have assumed that the bending magnets have a sector geometry, however, only small modifications usually result in the case of non-zero entrance and exit angles. In the special case of a lattice with parallel edged dipole magnets it may be shown that the effective field gradient at the entrance and exit of the magnet cancels the path length effect exactly, resulting in $D = 0$.

In separated function lattices therefore $J_x \sim 1$, $J_z = 1$ and $J_\varepsilon \sim 2$, and so the motion is damped in all three planes. This type of lattice is now generally used not only for storage rings, but also for synchrotrons since this also leads to smaller beam sizes. The difference between the two lattice types may be illustrated by the performance of the original DESY I synchrotron (combined function) and the later DESY II (separated function) [24], shown in Fig. 7. In DESY I the increase in horizontal beam size after an initial period of adiabatic damping is due to fact that the horizontal motion is anti-damped. A high repetition rate of 50 Hz was necessary in this case in order to limit the growth of the beam size. On the other hand, in DESY II the beam size approaches the equilibrium value even for widely different injected beam sizes and a much slower repetition rate could be used (12.5 Hz).

5.4 Damping time and injection energy

A common type of injection scheme for electron storage rings is multi-cycle injection, in which the injected beam damps in size due to radiation damping in the interval between injections so preventing loss on the injection septum magnet. In this way a high current can be

accumulated without needing a very high performance injector. The maximum possible injection rate depends to some extent on the damping time for the plane in which the injection is performed, usually the horizontal. This is particularly important when a ring is being filled at a lower energy than its final operating value since the damping time varies rapidly with energy, $\sim 1/E^3$.

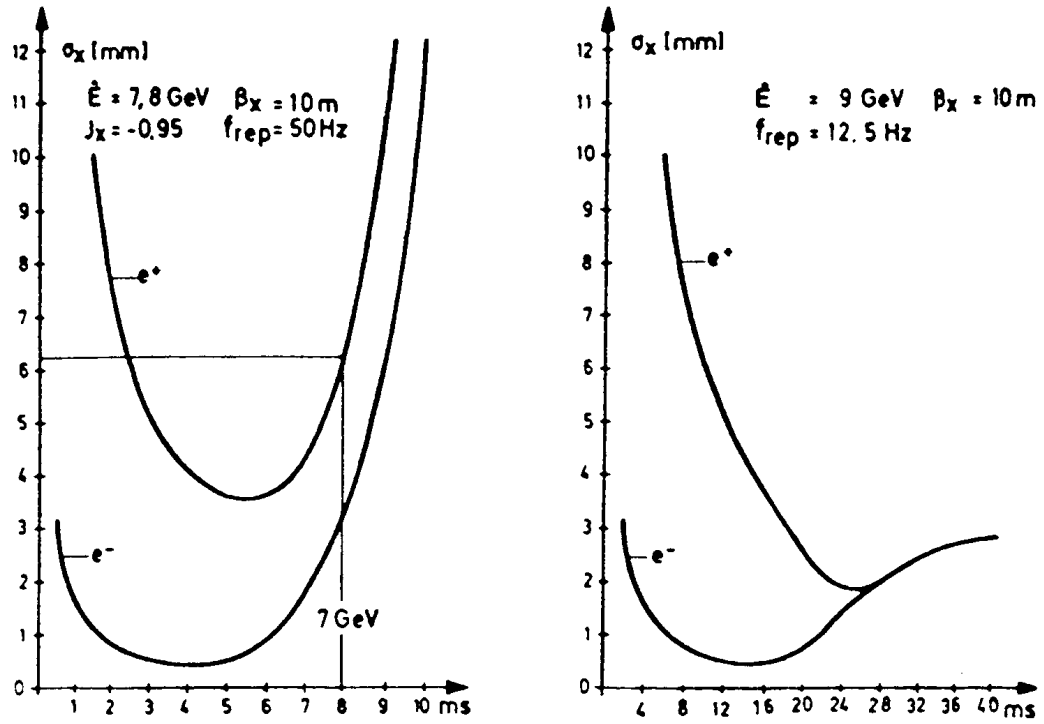

Fig. 7 Variation of horizontal beam size with time during the acceleration cycle in the DESY I (left) and DESY II (right) synchrotrons [24]

The importance of injection energy is illustrated by the unique system of beam storage that was employed at the CEA when it was operated as an electron storage ring with a low injection energy of 260 MeV [25]. In order to increase the current that could be accumulated the energy was cycled repeatedly between injection energy and 2.1 GeV, so that sufficient radiation damping could occur at the higher energy between successive injections.

The topic of injection energy is particularly relevant in the field of modern compact sources of synchrotron radiation [26]. Since the critical wavelength of the radiation at the operating energy varies as ρ/E_0^3, it follows that the same value can be obtained with a lower operating energy using superconducting magnets with a smaller bending radius than conventional magnets. This tends to reduce the overall circumference and so make the ring more compact. In addition, since the damping time at the injection energy varies as $T_0\rho/E_i^3$ it follows that a lower injection energy may be used while maintaining the same damping time, which permits a more compact and cheaper injector to be used.

Table 2

Damping times and injection rates in some electron storage rings with low energy multi-cycle injection

	COSY [29]	MAX [27]	ALADDIN [30]
Injection energy (MeV)	50	100	100
Damping time (s)	2.5	2.5	13.6

Injection rate (Hz)	10	10	1.25

Many other factors, however, affect the injection process at low energy, such as trapped ions, intra-beam scattering, instabilities etc., as well as complex beam dynamics [26,27], and the connection between damping time and injection rate is not well established. Table 2 gives data for three storage rings with a low energy injection, showing that multi-cycle injection can be achieved with a period as short as 1/25th of a damping time. At even lower energies a multi-cycle injection becomes impossible, however, it may be possible to inject sufficient current in a single shot. For example, the 600 MeV Super-ALIS ring in Japan can be injected in this way at only 15 MeV, where the radiation damping time is very long indeed (~ 4 min) [28].

6. MODIFICATION OF DAMPING RATES

In the following sections we consider various ways in which the damping rates can be modified in an existing lattice.

6.1 Gradient wiggler magnet

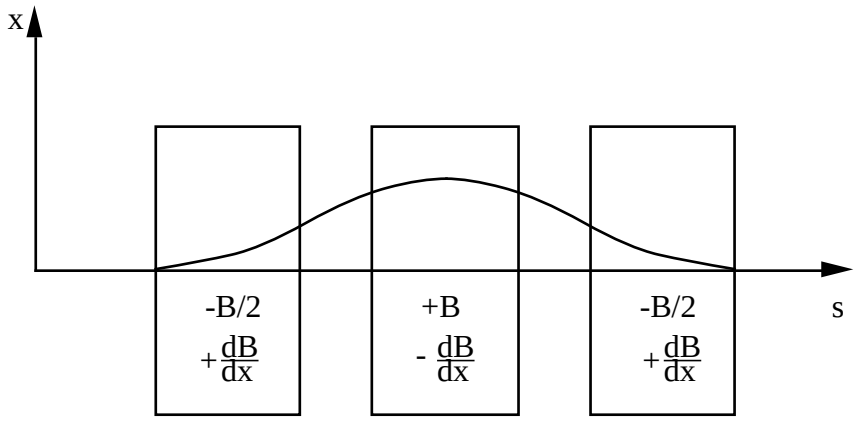

Fig. 8 Schematic diagram of a gradient wiggler magnet.

In order to modify the damping partition between the three planes a wiggler magnet with a gradient field may be used. This was first proposed by Robinson in 1958 as a means of overcoming the radial anti-damping of the CEA electron synchrotron, which has a combined function lattice [8,17]. For this reason it is often referred to as a "Robinson wiggler".

The method is to reduce the damping of the energy oscillation, thereby increasing the damping of the radial motion, by using a magnet in which higher energy electrons radiate less than lower energy electrons i.e. $dU/d\varepsilon$ is reduced. From Eq.(10) it can be seen that D reduces if $2kD/\rho > 0$ i.e. $DB(dB/dx) < 0$. A series of magnet poles with alternating polarity of dipole and gradient fields as shown in Fig. 8 will therefore achieve this. Such magnets were installed at CEA in order to permit operation as a storage ring [25,31] and also in the PS to permit operation with electrons [5]. The magnets used in the latter case are shown in Fig. 9.

Gradient wigglers have also been proposed as a means of decreasing the beam emittance in various synchrotron radiation sources, as will be discussed in the following Chapter.

6.2 Variation of r.f. frequency

Another technique that can be employed in large rings for modifying the damping partition numbers is variation of the r.f. frequency [20]. The effect of a change in frequency (f) is to cause the orbit length (L) to vary, so forcing the electrons to move onto an off-energy orbit:

$$\frac{\Delta f}{f} = -\frac{\Delta L}{L} = -\alpha\frac{\varepsilon}{E_0}$$

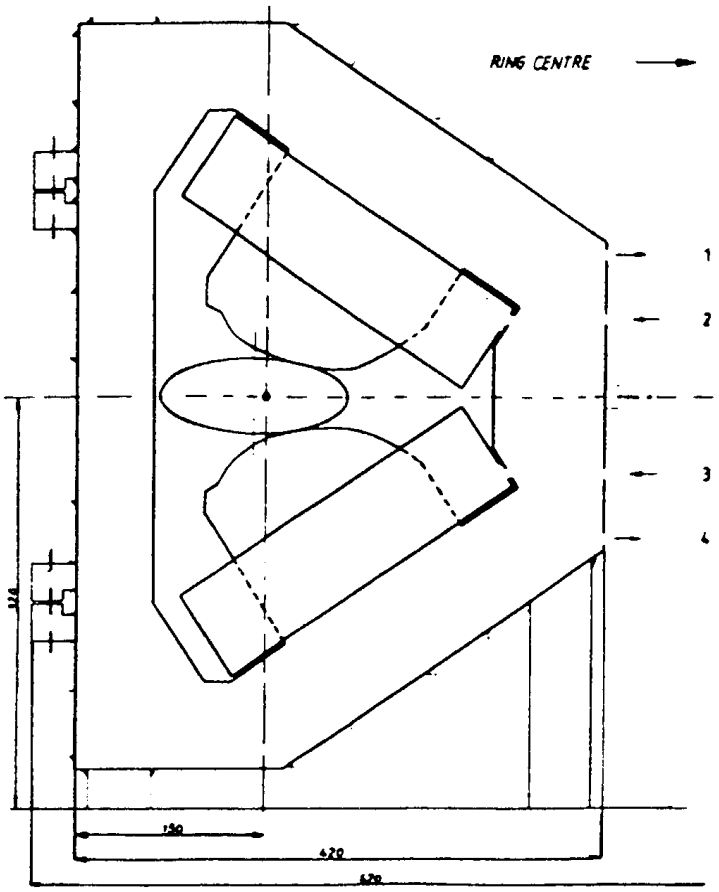

Fig. 9 Cross-section of the gradient wiggler magnet used in the PS [5]

where α is the momentum compaction factor. The shift in the orbit where there is finite dispersion, $x_\varepsilon = D(s)\,\varepsilon/E_0$, has various effects, the largest of which results from the dipole field seen by the particle in the quadrupole magnets, $(1/\rho)_{\text{quads}} = -kD\varepsilon/E_0$ [32]. It follows from Eq. (10) that there is a change in D given by:

$$\Delta D \cong \frac{\oint 2D^2k^2\varepsilon/E_0 ds}{\oint 1/\rho^2 ds}$$

Table 3 shows the magnitude of the effect for three rings of different size, expressed as the change in the horizontal damping partition number with energy deviation and with mean orbit radius ($R = L/2\pi$). It can be seen that in order to change J_x by unity the mean orbit position needs to be shifted by only 0.5 mm in LEP, with a corresponding energy deviation of only 0.13%, whereas in the EPA this change would require a movement of 30 mm, with an energy deviation of 5.6%. The method is effective therefore only in large rings; for example it was used regularly in PETRA [33] for luminosity optimization.

Table 3

Variation of horizontal damping partition number in various electron storage rings

	EPA [5]	PEP [34]	LEP [6]
$dJ_x/d(\varepsilon/E_0)$	-18	-100	-764
dJ_x/dR (mm^{-1})	-0.03	-0.26	-0.47

6.3 Betatron coupling

The techniques discussed in the above two sections both involve changing the damping partition between the horizontal betatron motion and the energy oscillations. Another possibility is to vary the partition between the horizontal and vertical planes by means of skew-quadrupole or solenoidal fields, without affecting the energy oscillations. This was one of the additional techniques originally proposed as a means of overcoming the radial anti-damping in combined function lattices [8,20].

6.4 Dipole wiggler magnet

It follows from Eq. (16) that an increase in the energy loss per turn U_0 will bring about an increase in all three damping rates. This can be achieved using a series of magnets with alternating polarity, arranged so that there is no net deflection of the electron beam as shown in Fig. 8, but in this case without the gradient field. Such a device is known as a dipole wiggler, or alternatively as a damping wiggler. A dipole wiggler also affects the equilibrium between the radiation damping and quantum excitation processes and so modifies the emittance in a complicated way, depending on the ring energy, wiggler parameters and the dispersion function, and will be discussed further in the following Chapter. Dipole wigglers are in operation in LEP and Fig. 10 shows the design of the magnets that are used [35].

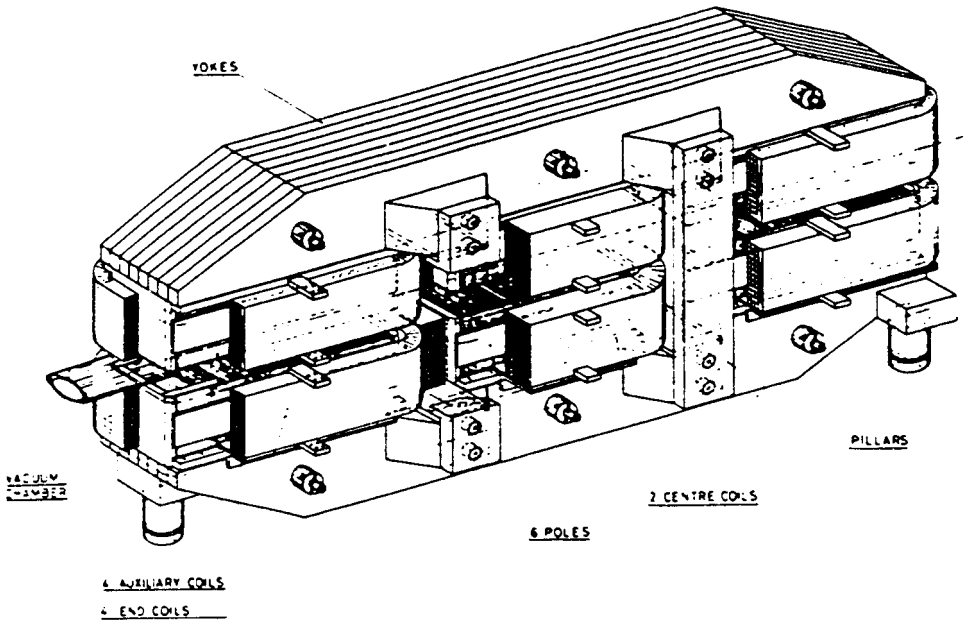

Fig. 10 The dipole wiggler magnet design for LEP [35]

7. MEASUREMENT OF DAMPING RATES

In general, the damping rates are of less interest as compared with other parameters, such as for example beam sizes and bunch lengths, and for this reason there are few published reports about such measurements. Several measurements have however been made at the SLC damping rings, whose performance depends very much on the damping rate. In one experiment the sum of the three damping rates was inferred indirectly by measuring the energy loss per turn U_0 (Eq. (16)) [36]. This was done by using the relation $U_0 = V_{rf} \sin(\phi)$, by measuring the peak accelerating voltage (V_{rf}) and the phase angle (ϕ), extrapolated to zero

current. The damping time was also obtained by measuring the variation of the extracted beam size as a function of storage time. More recently a synchrotron light monitor was used with a fast gated camera to directly measure the beam size as a function of time after injection. Figure 11 shows a typical result [37].

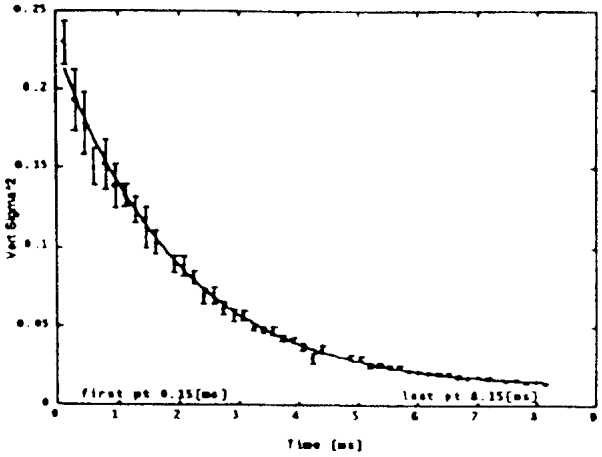

Fig. 11 Variation of the beam size in the SLC electron damping ring as a function of time after injection [37]

By fitting the data with an expession of the form:

$$\sigma_\beta^2 = \sigma_{\beta i}^2 \exp\left(-\frac{2t}{\tau}\right) + \sigma_{\beta o}^2\left[1 - \exp\left(-\frac{2t}{\tau}\right)\right],$$

where $\sigma_{\beta 0}$ is the r.m.s. equilibrium beam size and $\sigma_{\beta i}$ is the inital value after injection, the damping times in both horizontal and vertical planes (τ_x and τ_z)were obtained.

A similar method was used also in the EPA to measure the horizontal and vertical damping rates. In this case a stored beam was excited with a fast kicker magnet and the changing beam profile observed with a synchrotron radiation beam profile monitor [38]. Figure 12 shows a sample result, from which the damping time may be extracted using the expression above, with $\sigma_{\beta i}$ equal to the inital value after the blow-up using the kicker magnet (assuming zero dispersion at the measurement point).

For the longitudinal damping rate there is the possibility of making the same observations as above in the horizontal plane but at a point with large dispersion. This is because the total beam size contains contributions from the betatron motion and the energy spread, $\sigma^2_{\text{total}} = \sigma^2_\beta + D^2(\sigma^2_\varepsilon/E_0^2)$ with different damping rates, τ_x and τ_ε respectively. Alternatively, some form of r.f. excitation could be applied and the resulting changes in the bunch length could be measured directly using an appropriate electron beam pick-up or synchrotron light monitor system.

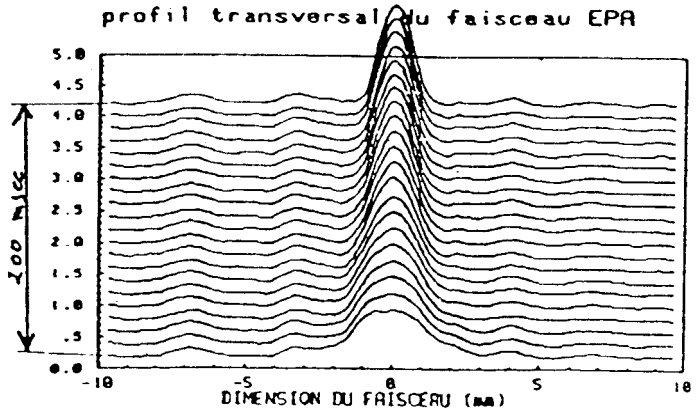

Fig. 12 Variation of the transverse profile of the beam in EPA after excitation with a fast kicker magnet [38]

REFERENCES

[1] M. Sands, SLAC-121 (1970).

[2] S. Krinsky, M.L. Perlman and R.E. Watson, "Characteristics of Synchrotron Radiation and its Sources", Handbook on Synchrotron Radiation, Vol. Ia, North Holland, 1983.

[3] K. Hübner, Proc. CERN Accelerator School, General Accelerator Physics, CERN 85-19, Nov. 1985, p. 239.

[4] J. Le Duff, These proceedings.

[5] LEP Design Report, Vol.1, The LEP Injector Chain, CERN-LEP/TH/83-29, June 1983.

[6] LEP Design Report, Vol.2, The LEP Main Ring, CERN-LEP/84-01, June 1984.

[7] J.M. Jowett, AIP Conference Proceedings 153, Vol.1, Physics of Particle Accelerators, American Inst. Phys. (1987) p. 864.

[8] K.W. Robinson, Phys. Rev. 111 (1958) 373.

[9] Advanced Engineering Mathematics, E. Kreyszig, John Wiley (1988).

[10] K. Steffen, Ref. 3, p. 25.

[11] N.H. Frank, Phys. Rev. 70 (1946) 177.

[12] D. Bohm and L. Foldy, Phys. Rev. 70 (1946) 249.

[13] J. Schwinger, Phys. Rev. 70 (1946) 798.

[14] G. Rakowsky and L.R. Hughey, IEEE Trans. Nucl. Sci. NS-26 (1979) 3845.

[15] H. Yamada, J. Vac. Sci. Technol. B8, (1990) 1628.

[16] A.A. Kolomenski and A.N. Lebedev, CERN Symposium (1956) p. 447.

[17] M.S. Livingston, CERN Symposium (1956) p. 439.

[18] I.G. Henry, Phys. Rev. 106 (1957) 1057.

[19] Yu.F. Orlov et. al., Proc. Int. Conf. High Energy Accelerators, CERN (1958) p. 306.

[20] H.G. Hereward, Proc. Int. Conf. High Energy Accelerators, Brookhaven (1961) p. 222.

[21] A. Hofmann and B. Zotter, IEEE Trans. Nucl. Sci. NS-24 (1977) 1875.

[22] L. Mango, Frascati National Laboratory, LNF-62/34, May 1962.

[23] F.E. Mills, Nucl. Instr. Meth. 23 (1963) 197.

[24] G. Hemmie, IEEE Trans. Nucl. Sci. NS-30 (1083) 2028.

[25] H. Winick, IEEE Trans. Nucl. Sci., NS-20 (1973) 984.

[26] E. Weihrehter, Proc. 3rd European Particle Accelerator Conference, Berlin, March 1992, Editions Frontieres (1992), p. 93.

[27] M. Eriksson, Nucl. Instr. Meth. Phys. Res. A291 (1990) 461.

[28] T. Hosokawa et. al., Rev. Sci. Instr. 60 (1989) 1783.

[29] E. Weireter et. al., Proc. 2nd European Particle Accelerator Conference, Nice, June 1990, Editions Frontieres (1990), p. 237.

[30] E.M. Rowe, Proc. 1987 US PArticle Accelerator Conference, IEEE CH2387-9/87/0000-0391, (1987) p. 391.

[31] A. Hofmann et. al., Proc. 6th Int. Conf. High Energy Accelerators, Cambridge, 1967, p. 123.

[32] J.P. Delahaye and J. Jäger, SLAC-PUB-3585, February 1985.

[33] A Piwinski, IEEE Trans. Nucl. Sci, NS-30 (1983) 2378.

[34] M. Donald et al, SSRL-ACD-Note 42, December 1986.

[35] J.M. Jowett and T.M. Taylor, IEEE Trans. Nucl. Sci. NS-30 (1983) 2581.

[36] L. Rivkin et al, IEEE Trans. Nucl. Sci. NS-32 (1985) 2626.

[37] F.J. Decker et. al., Proc. 3rd European Particle Accelerator Conference, Berlin, March 1992, Editions Frontières, p. 342.

[38] J.F. Bottollier and J.P. Delahaye, CERN PS/LPI Note 87-11, March 1987.